System Identification Applied to Spatial and Temporal Propagation of Atrial Activity During Atrial Fibrillation

Santos, Susana; Carlson, Jonas; Olsson, Bertil; Johansson, Rolf

Published in:
Proceedings of the 40th IEEE Conference on Decision and Control, 2001.

DOI:
10.1109/.2001.980213

2001

Proceedings of the 40th IEEE
Conference on Decision and Control
Orlando, Florida USA, December 2001

System Identification Applied to Spatial and Temporal Propagation of Atrial Activity During Atrial Fibrillation

Susana Santos[1] Jonas Carlson[2] Eva Hertervig[2] Bertil Olsson[2] Rolf Johansson[1]
[1]Department of Automatic Control, Lund Institute of Technology
PO Box 118, SE-221 00, Lund, Sweden
{susana|Rolf.Johansson}@control.lth.se
[2]Department of Cardiology, Lund University, SE-221 85 Lund, Sweden
{Jonas.Carlson|Eva.Hertervig|Bertil.Olsson}@kard.lu.se

Abstract

The purpose of this paper is to apply system identification methods to study spatial and temporal propagation of atrial activation along coronary sinus (situated in the posterior left part of the heart, in the groove between left atrium and left ventricle) during paroxysmal atrial fibrillation (PAF) using data recorded catheter from 7 different patients. Furthermore, interatrial mechanisms of impulse conduction can be derived due to the position of coronary sinus. This study demonstrated consistency in electrical activity propagation during atrial fibrillation (AF) along coronary sinus in five patients out of six included. Nevertheless, results on direction and speed of propagation depended on the patient. For reference purposes, the method was tried out during sinus rhythm (SR) obtaining the expected high consistency in propagation direction and speed.

Introduction

Despite the fact that atrial fibrillation is one of the most common cardiac arrhythmias in man, the mechanisms maintaining this arrhythmia have not yet been satisfactorily clarified. In 1962, Moe presented his 'multiple wavelet hypothesis' to explain the characteristics of atrial fibrillation [1]. According to this hypothesis, atrial fibrillation is maintained by the coexistence of a number of independent activation waves, called wavelets, that travel randomly through the atrial myocardium around multiple islets or strands of non-excitable tissue.

By endocardial activation mapping, Allessie and coworkers have confirmed Moe's hypothesis as a basis of acetylcholine-induced atrial fibrillation in isolated canine hearts [2,3], [5]. They identified three types of right atrial activation patterns, characterized by different properties of the intra-atrial re-entrant circuits.

Cox *et al.* included epicardial activation mapping of electrically induced atrial fibrillation both in dogs with created mitral regurgitation and in patients with Wolff-Parkinson-White syndrome [4], [5]. The whole epicardial surface of both the right and the left atria was mapped using 208 electrodes in the animal set-up and 160 electrodes in the clinical set-up. The study demonstrated that multiple wave fronts, nonuniform conduction, bidirectional block and large re-entrant circuits occurred during induced atrial fibrillation.

Temporal averaging as well as characteristization of the individual beats and atrial activations have been developed applying a state-space realization technique in order to fit a multivariate impulse response model to data from multiple simultaneously acquired atrial electrograms [6,8,9]. Although the methods [6,8,9] have proven to be reliable tools for identifying atrial areas with consistent activation during fibrillation and electrograms have been locally and successfully predicted [8], it remains a relevant issue to evaluate spatiotemporal organization of arrhythmia.

During direct impulse conduction, using cardiac catheters and electrical stimulation technique, we observed that patients prone to attacks of atrial fibrillation often had evidence of delayed impulse conduction between the right and the left atrium, the mechanisms causing this delay being unknown [7]. As the catheter is placed in the posterior left part of the heart, in the groove between left atrium and left ventricle, with one pole in the orifice of coronary sinus inside right atria, mechanisms of impulse conduction between right and left atria can be derived.

The purpose of this paper is to present results on spatial and temporal propagation of atrial activation along coronary sinus during paroxysmal atrial fibrillation in different patients.

0-7803-7061-9/01/$10.00 © 2001 IEEE

Materials and Methods

Seven patients with paroxysmal atrial fibrillation (PAF) were included in the study, six of them measured during PAF and one measured during sinus rhythm (SR). The clinical characteristics of the patients are shown in Table 1. No anesthesia was used except Diazepam 2.5-5mg intravenous injection when needed. Endocardial electrograms were simultaneously acquired with a commercially available standard 10 polar catheter placed in the coronary sinus (cs). The closest pole to right atrium is in the orifice of coronary sinus (Pole number 10). This catheter was always motivated by the clinical procedure. A DAIG 6F Decapolar CSL catheter (catalogue number 401400) was used in the first 6 patients, measured during PAF. Each pole was 1 mm wide and the distance between the electrodes 5 mm. Therefore, the average distance between electrodes was considered 6 mm. For Patient 7, measured during SR, a BARD 6F Decapolar Dynamic XT (catalogue number 201101) was used, with electrode average spacing 2, 5, 2 mm alternatively.

Also, 12-lead body surface recordings (surface-ECG) were made using commercially available standard ECG electrodes. Only lead V1 was used in this study as a reference to distinguish ventricle and atrial activation in endocardial electrograms. Each recording consisted of 10 unipolar electrograms from cs and lead V1 surface-ECG, simultaneously acquired with a sampling rate of 1 kHz, unfiltered and A/D converted with a resolution of 12 bits. The catheter was connected to the BARD Cardiac Mapping System for data acquisition (Table 2). First three patient recordings were acquired with the following protocol: the first 30 seconds and the last 30 seconds were obtained with no artificial pacing but the remainder 30 seconds in between were measured while artificial atrial pacing performed at a pacing rate of 25 ms less than the mean interval of atrial fibrillation (measured during one minute) using two poles (1-2, 5-6 or 9-10) of the coronary sinus catheter connected to an external heart stimulator. Recordings during pacing were not used in this study. Recordings from Patients 4, 5 and 6 were acquired without any artificial pacing.

After visual analysis of each data set, some intervals of data have been manually discarded due to saturated signals when pole-tissue contact is not complete. Moreover, data very close to the end of the artificial pacing has also been rejected during the interval that signals from pacing poles did not reach their mean value. Besides, removal of a 50 Hz disturbance component emanating from power supplies was applied.

Table 1: Clinical Characteristics of the patients.

Patient	*Sex M/F*	*Age (years)*	*Cardial Rhythm*
1	M	52	PAF
2	M	22	PAF
3	M	56	PAF
4	M	48	PAF
5	M	46	PAF
6	M	50	PAF
7	F	58	SR

PAF= Paroxysmal Atrial Fibrillation.

Correlation analysis on complete signals

We computed the correlation function among signals along the coronary sinus catheter, the correlation function between two signals being defined as

$$\rho(\tau) = \frac{C_{xy}(\tau)}{\sqrt{|C_{xx}(\tau)|}\sqrt{|C_{yy}(\tau)|}}, \tau = -n, \ldots, -1, 0, 1, \ldots, n$$

The time shift τ ms considering sampling rate equal to 1 kHz The sample covariances are defined as

$$C_{xy}(\tau) = \frac{1}{N-\tau}\sum_{i=1}^{N-\tau}(x_{i+\tau} - \bar{x}_{1+\tau,N})(y_i - \bar{y}_{1,N-\tau})^T \quad (1)$$

and the sample means

$$\bar{x}_{1,N-\tau} = \frac{1}{N-\tau}\sum_{i=1}^{N-\tau} x_i, \quad \bar{x}_{1+\tau,N} = \frac{1}{N-\tau}\sum_{i=1+\tau}^{N} x_i$$

where:

N= total number of samples

τ= time shift in ms.

Next, the maximum of the correlation function is

$$\tau_{\max} = \arg\max_{\tau}(\rho(\tau)), \quad \rho_{max} = \rho(\tau_{max}) \quad (2)$$

where τ_{max} gives the time shift (in miliseconds) where both signals are most correlated, i.e., major similarity between these two signals is found when one of them is shifted τ *ms.* and ρ_{max} gives the maximum correlation coefficient in a range from zero to one which means that correlation between signals is low or high, respectively.

Excitation direction and velocity component

All signals were analyzed in order to find the reference signal as the one that presented first activation by means of resulting positive time shifts in the maximum of the correlation function. coronary sinus can be extracted. The *excitation direction* can be inferred from the sign of τ_{max}. A positive time shift indicated

Table 2: Characteristics of recordings for each patient.

Patient	*Poles included*	*Pacing poles*	*Duration NP + P (seconds)*
1	all	1-2	58+32
1	all	5-6	60+31
1	all	9-10	60+30
2	all	1-2	66+29
2	all	5-6	61+30
2	all	9-10	60+30
3	all	1-2	62+31
3	all	5-6	62+31
4	4,6,8,10	none	42+0
5	1,4,6,8,10	none	11+0
5	1,4,6,8,10	none	28+0
6	1,4,6,8,10	none	14+0
7	all	none	64+0
7	all	none	65+0

NP= Time (s) of recordings without artificial pacing.
P= Time (s) of recordings during artificial pacing between electrodes shown in column 'Pacing Poles'.

propagation from the reference pole to the other pole used to calculate the correlation function, whereas a negative time shift denotes propagation towards the reference signal. The *excitation speed* can be estimated from the absolute value of τ_{max}.

$$v_{r,x} = \frac{6|x-r|}{(\tau_{max})_{r,x}} \frac{m}{s} \tag{3}$$

r = index of reference pole
x = index of second pole in correlation function
$(\tau_{max})_{r,x}$ = maximum in the correlation function between signals from poles r and x.

Substitution of ventricle response by a linear interpolation in all CS catheter signals
Considering that ventricular excitation affected our signals with higher amplitude than atrial excitation, previous results could be distorted by ventricular activity. Since we are only interested in atrial electrical activity, substitution of ventricle response was performed calculating its start and end as the limits of the QRS complex in lead V1 surface-ECG. Interpretation of ECG recordings traditionally classify the signal morphology in terms of P-wave (atrial activation) followed by a QRS complex (ventricle activation). Accurate estimation of QRS start and end was not necessary as long as the high magnitude of ventricle impulse is removed from the coronary sinus signals. Afterwards, a linear interpolation was calculated in between both estimated limits. An example of this substitution is presented in Figs.1 and 2 during one heart beat. Large difference in magnitude of ventricle and atrial response can be recognized.

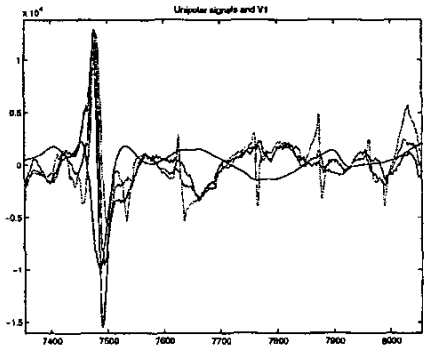

Figure 1: Real signals during one heart beat in Patient 3. Lead V1 surface-ECG (black) and coronary sinus signals from Poles 1-3 (colored).

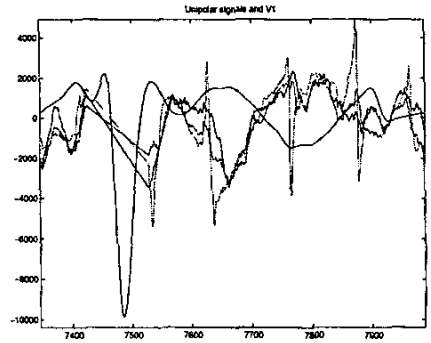

Figure 2: Signals with ventricle response removed during one heart beat in Patient 3. Lead V1 surface-ECG (black) and coronary sinus signals from Poles 1-3 (colored).

System identification for cross verification
Considering as inputs the closest poles to the output electrode, a simple linear model was fitted to data using least-squares method. The input-output delay was given by the results obtained from the correlation analysis. Our linear regression analysis is based on the model

$$y_{k,s} = \sum_{i=1}^{N} a_i y_{k-i,s} + \sum_{i=d_1}^{N} b_i y_{k-i,s-1} + \sum_{i=d_2}^{N} c_i y_{k-i,s+1} + e_k \tag{4}$$

where:
s = space (number output pole)
k = time (sample instant)
d_1 = delay between y_s and y_{s-1} given by previous results in correlation analysis
d_2 = delay between y_s and y_{s+1} given by previous results in correlation analysis
e_k = additive errors are assumed to have the form:

$$E\{e_i\} = 0, \quad E\{e_i e_j\} = \sigma_e^2 \delta_{ij}, \quad \forall i,j \tag{5}$$

In ARX form

$$A(q)y_s(t) = B(q)y_{s-1}(t-d_1) + C(q)y_{s+1}(t-d_2) \quad (6)$$

Model validation was quantitatively computed in terms of percentage 'Variance Accounted For' (VAF) and qualitatively by cross validation between real and estimated output.

$$\text{VAF} = (1 - \frac{(\mathcal{Y}_N - \hat{\mathcal{Y}}_N)^T(\mathcal{Y}_N - \hat{\mathcal{Y}}_N)}{\mathcal{Y}_N^T\mathcal{Y}_N}) \times 100\% \quad (7)$$

The VAF score is a simple test quantity which gives a measure of the correctness of a model by comparing the estimated output of the model and output data. Cross validation was made applying input data not previously used in identification to investigate the fit of model and data.

In summary, the procedure used involved 1) preprocessing and QRS cancellation 2) correlation analysis and 3) lead ordering with estimation of delays and speeds.

Results

Results in correlation analysis showed consistent patterns in spatial and temporal propagation during atrial fibrillation in five patients out of six. Two wave fronts meeting somewhere inside the coronary sinus were identified in Patients 1 and 2. For example, Fig. 3 presents the correlation function for Patient 2 where the maximum spreads out in space (1st to 8th Pole in the catheter) increasing time shift from 0 to 45 ms and then decreasing again (from 8th to 10th Pole). Consequently, two different excitation directions were obtained confronting in Pole 8. A unique consistent wave was found in Patients 3, 4 and 5. Fig. 3 shows results for Patient 3 where only one propagation direction appeared from 7th to 1st Pole increasing time shift from 0 to 33 ms. No consistent spatial propagation was obtained for the last AF Patient.

Direction and speed of propagation resulted dependent on the patient (Table 3). During sinus rhythm, the case presented higher values in the maximum of the correlation function than during AF and a unique wave as it is shown also in Table 3.

The models obtained exhibited high accuracy and low order (model order 4-6). Results of typical experimental data and cross-validation simulation are presented in Fig. 4 (Patient 3, AF, 1 wave front, VAF= 83,4%) and Fig. 5 (Patient 7, SR, VAF= 97,9%).

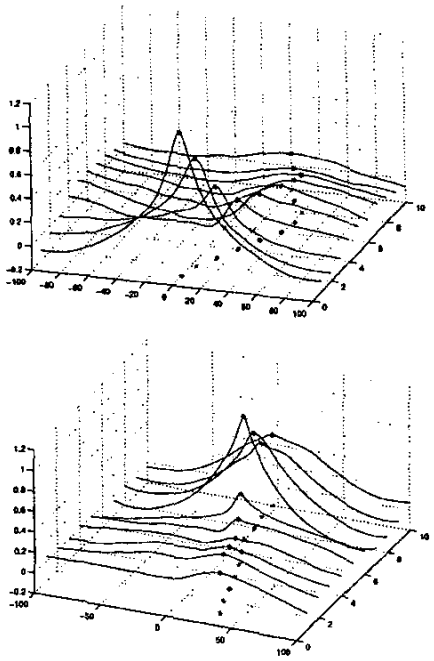

Figure 3: Correlation function (*Upper graph:* Patient 2, interval 1, between first pole as reference and all the others.) Correlation function (*Lower graph:* Patient 3, interval 3, between 7th Pole and all the others.) The maximum of each correlation function is shown as a * over the function and also its projection. X axis represents space: 1st to 10th Poles in the catheter. Y axis represents time shift and Z axis gives the value of the correlation coefficient.

Discussion

This study demonstrated consistency in electrical activity propagation during atrial fibrillation along coronary sinus in all cases with one exception.

The findings regarding to two wave fronts in first two patients are compatible with excitation that follows the same patterns as expected during SR, i.e., one wave front propagating from the roof of the left atrium and the other one coming from the right atrium by inferoposterior interatrial connections running in bundles or in the wall of coronary sinus. This is evidence of left atrial activation from right atrium during PAF. In any case, all results can be used to derive mechanisms of impulse conduction between right and left atrium due to the position of coronary sinus.

However, speed calculations were not conclusive due to signals being spatially limited to one dimension but no information is acquired from the other two

Table 3: Maximum correlation coefficient range, excitation direction and speed in each data interval.

Patient/ Data interval	*Interval Duration (ms)*	ρ_{max} *range*	*Excitation direction*	*Excitation speed (m/s)*
1/1	30840	0.91 to 0.5	$1 \Leftarrow 2-3 \Rightarrow 8-9 \Leftarrow 10$	X/1.15/X
1/2	12014	0.93 to 0.45	$1 \Leftarrow 2-3 \Rightarrow 8-9 \Leftarrow 10$	X/1.11/X
1/3	15801	0.95 to 0.55	$1 \Leftarrow 2-3 \Rightarrow 7 \Leftarrow 8-9-10$	X/1.5/X
1/4	24401	0.96 to 0.49	$1-2-3 \Rightarrow 7 \Leftarrow 10$	1.1/0.82
1/5	6501	0.95 to 0.23	$1 \Leftarrow 2-3 \Rightarrow 7 \Leftarrow 10$	X/1.2/0.9
2/1	33701	0.68 to 0.08	$1 \Rightarrow 8 \Leftarrow 10$	0.93/0.63
2/2	8601	0.63 to 0.07	$1 \Rightarrow 8 \Leftarrow 9-10$	0.78/X
2/3	29800	0.52 to 0.15	$1 \Rightarrow 7 \Leftarrow 9-10$	1.16/1.33
2/4	8564	0.51 to 0.06	$1 \Rightarrow 6-7 \Leftarrow 10$	0.94/1
2/5	28752	0.59 to 0.11	$1 \Rightarrow 7-8$ *	0.78
3/1	23201	0.53 to 0.3	$1 \Leftarrow 5$	0.92
3/2	18251	0.54 to 0.16	$1 \Leftarrow 5$	0.6
3/3	29500	0.7 to 0.2	$1-2 \Leftarrow 7-8$	1.09
3/4	24960	0.76 to 0.16	$1 \Leftarrow 7-8$	0.77
4/1	19801	0.16 to 0.08	$4 \Leftarrow 10$	0.9
4/2	19701	0.22 to 0.07	$6 \Leftarrow 10$	0.92
5/1	5000	0.32	$4 \Rightarrow 6$	0.8
5/2	9464	0.23	$4 \Rightarrow 6$	0.92
6/1	11775	0.86 to 0.11	no patterns	X
6/2	28287	0.9 to 0.26	no patterns	X
7/1	19851	0.91 to 0.6	$1 \Leftarrow 8-9-10$	0.71
7/2	20001	0.94 to 0.65	$1 \Leftarrow 8-9-10$	0.71
7/3	23993	0.94 to 0.66	$1 \Leftarrow 8-9-10$	0.71
7/4	20001	0.95 to 0.66	$1 \Leftarrow 8-9-10$	0.71
7/5	28001	0.93 to 0.65	$1 \Leftarrow 8-9-10$	0.71
7/6	6866	0.95 to 0.68	$1 \Leftarrow 8-9-10$	0.74

Numbers 1 to 10 denote pole numbers in the coronary sinus catheter;
$\Leftarrow, \Rightarrow$: give the consistent direction patterns in propagation;
x-y :no time shift between x and y electrodes or smaller than 3 ms.
speed1/speed2 :each speed corresponds to each previous direction (arrow);
X:speed calculation impossible; *: Poles 9 and 10 saturated.

dimensions in space. Therefore, electrical activity propagating in an oblique direction towards coronary sinus will produce an erroneous speed calculation. Interesting future work could be done applying the same procedure on signals spread out inside the atria in two and three dimensions, which was infeasible at the moment of the study due to limitations in available catheters. The validity of the method was enhanced looking into the results during sinus rhythm. The normal cardiac rhythm is initiated from sinus node, close to the entrance of the superior caval vein into the right atrium, then it propagates along the entire myocardium. The *direction and speed of excitation* obtained in our study confirmed the expectations from previous studies [7,10,11]. Furthermore, elevated maximum correlation coefficients, compared to those obtained during AF, showed high consistency in propagation, as it is known during sinus rhythm.

High accuracy in resulting models manifested linear relation among signals in the coronary sinus catheter. In addition, cross validation simulation showed our system, electrical propagation among electrodes, was time invariant during intervals belonging to the same data set and patient. The manifested linear and time invariant relation among unipolar signals could stimulate future research in building models of electrical activity inside the heart during different basal rhythms.

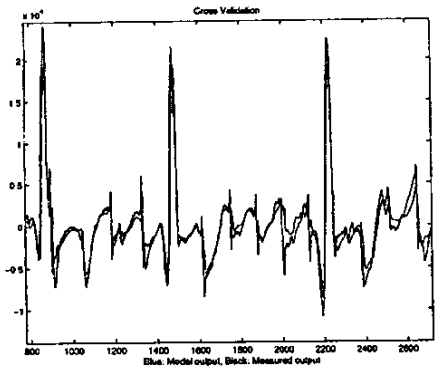

Figure 4: Accuracy of cross validation, Patient 3, AF. Output: 7th Pole, Inputs: 6th and 8th Poles, order=5, VAF= 83,4%.

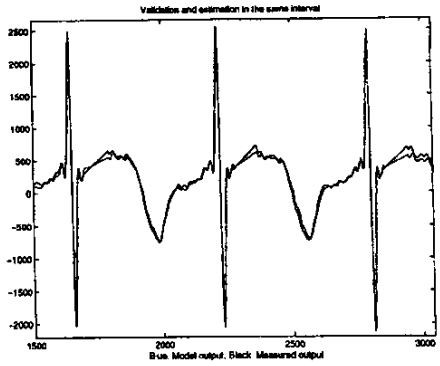

Figure 5: Accuracy of cross validation, Patient 7, SR. Output: 7th Pole, Inputs: 6th and 8th Poles, order=4, VAF= 97,9%.

Conclusions

Despite the fact that different wave front directions have been found, depending on the patient, we have demonstrated consistency in electrical activity propagation during atrial fibrillation along coronary sinus in all cases with only one exception. This could lead to future interpretations and work applying the same procedure on signals spread out inside the atria, ideally in three dimensions, where no ventricle response can distort atrial activations for analysis. However, we have tested our procedure on signals during sinus rhythm obtaining the expected results in speed and direction of excitation as well as high consistency in patterns.

Acknowledgments

This work was made while the first author was on leave from Departamento de Sistemas y Automatica, Universidad de Valladolid, Spain. The authors thank Prof. Enrique Baeyens for cooperation.

References

[1] G. K. Moe. On the multiple wavelet hypothesis of atrial fibrillation. *Arch Int. Pharmacodyn Ther*, 140:183–188, 1962.

[2] M. A. Allessie, W. J. E. P. Lammers, F. I. M. Bonke, and J. Hollen. Experimental evaluation of Moe's multiple wavelet hypothesis of atrial fibrillation. In D. P. Zipes and J. Jalife, editors, *Cardiac arrhythmias*, pages 265–275. Grune and Stratton, NY, 1985.

[3] K. T. S. Konings, C. J. H. J. Kirchhof, J. R. L. M. Smeets, H. J. J. Wellens, O. C. Penn, and M. A. Allessie. High-density mapping of electrically induced atrial fibrillation in humans. *Circulation*, 89(4):1665–1680, 1994.

[4] J. L. Cox, T. E. Canavan, R. B. Schuessler, M. E. Cain, B. D. Lindsay, C. Stone, P. K. Smith, P. B. Corr, and J. P. Boineau. The surgical treatment of atrial fibrillation II. Intraoperative electrophysiologic mapping and description of the electrophysiologic basis of atrial flutter and atrial fibrillation. *J. Thorac. Cardiovasc. Surg.*, 101:406–426, 1991.

[5] E. P. Gerstenfeld, A. V. Sahakian, and S. Swiryn. Evidence for transient linking of atrial excitation during atrial fibrillation in humans. *Circulation*, 86:375–382, 1992.

[6] M. Holm, R. Johansson, S. B. Olsson, J. Brandt, and C. Lührs. A new method for analysis of atrial activation during chronic atrial fibrillation in man. *IEEE Trans. Biomedical Engineering*, 43(2):198–210, February 1996.

[7] P.G. Platonov, S. Yuan, E. Hertervig, O.Kongstad, A. Roijer, A. B. Vygovsky, L.V. Chireikin, and S.B. Olsson. Further evidence of localized posterior interatrial conduction delay in lone paroxysmal atrial fibrillation. *Europace*, 3, January 2001.

[8] R. Johansson, M. Holm, S. B. Olsson, and J. Brandt. System identification of atrial activation during chronic atrial fibrillation in man. *IEEE Transactions on Automatic Control*, 43(6):790–799, June 1998 1998.

[9] M. Holm, R. Johansson, J. Brandt, C. Lührs, and S. B. Olsson. Epicardial right free wall mapping in chronic atrial fibrillation—documentation of repetitive activation with a focal spread—a hitherto unrecognized phenomenon in man. *European Heart Journal*, 18(2):290–310, February 1997.

[10] P.G. Platonov, J. Carlson, M.P. Ingemansson, A. Roijer, A.Hansson, L.V. Chireikin, and S.B. Olsson. Detection of inter-atrial conduction defects with unfiltered signal-averaged P-wave ECG in patients with lone atrial fibrillation. *Europace*, 2:32–41, January 2000.

[11] F. Roithinger, J. Cheng, and A. SippensGroenewegen et al. Use of electroanatomic mapping to delineate transseptal atrial conduction in humans. *Circulation*, 100:1791–1797, 1999.

[12] R. Johansson. *System Modeling and Identification*. Prentice Hall, Englewood Cliffs, NJ, 1993.